

Deactivating effect of coke and basic nitrogen compounds during the methylcyclohexane transformation over H-MFI zeolite

G. Caeiro^{a,b}, P. Magnoux^b, P. Ayrault^b, J.M. Lopes^a, F. Ramôa Ribeiro^{a,*}

^a Centro de Engenharia Biológica e Química, Instituto Superior Técnico, Av. Rovisco Pais, 1049-001 Lisbon, Portugal

^b Laboratoire de Catalyse en Chimie Organique, UMR 6503, 40 avenue du Recteur Pineau, 86022 Poitiers Cedex, France

Abstract

In this research work the deactivation of an H-MFI ($\text{Si}/\text{Al}_{\text{fr}} = 12$) zeolite was studied during the methylcyclohexane transformation at 350 °C. Besides the normal activity decay with time on stream due to the formation of coke molecules, the poisoning with three nitrogen basic compounds (3-methylpyridine, quinoline and 2,6-dimethylpyridine) was studied. All three bases cause a strong decrease in conversion. The decrease in activity is proportional to the amount of nitrogen retained in the zeolite. On the other hand, the intrinsic poisoning effect of the bases seems to correlate well with its proton affinity, following the order: 2,6-dimethylpyridine > quinoline > 3-methylpyridine. Although the relatively small pores of the MFI structure, until a saturation amount, the total injected amount of nitrogen bases stays in the zeolite in the protonated form. Even so, results show that the bulkier base cannot penetrate as deep into zeolites crystallites and accumulates on the external surface which can partially explain its higher poisoning ability. Besides the actual bases, no nitrogen coke molecules were found by GC–MS coupling; soluble coke molecules were polyaromatics with 2–4 rings.

© 2006 Elsevier B.V. All rights reserved.

Keywords: H-MFI zeolite; Cracking; Methylcyclohexane; Nitrogen; 3-Methyl-pyridine; Quinoline; 2,6-Dimethyl-pyridine; Poisoning; Deactivation; Coke

1. Introduction

Fluid catalytic cracking (FCC) is one of the most important processes in oil refining, its main goal is to produce gasoline. Two zeolites are used in FCC: Y (mainly in its ultra-stabilized form—USY) zeolite and MFI (or ZSM-5). The last one is used as an additive to the main catalyst. At first, its utilization aimed at improving the octane number of gasoline, primarily by favoring the cracking and isomerization of the low-octane compounds into lighter and more branched products [1–3]. Nowadays, refiners also want to enhance the production of light olefins, notably propene [4]. The demand for this product is increasing rapidly due to the expanding market for polypropylene. Besides, LPG-range olefins can be used as feedstock for alkylation and isomerization units where clean, high octane gasoline components and other chemicals are produced. Another important application of the light olefins is in the production of oxygenated antiknock gasoline additives, mainly methyl *tert*-butyl ether (MTBE) and *tert*-amyl methyl ether (TAME).

MFI is an intermediate pore zeolite which has a three-dimensional structure constituted by two types of channels, both delimited by 10 oxygen atom rings. The first ones are straight and run parallel to [0 1 0], its dimensions are 5.3 Å × 5.6 Å. The second ones are sinusoidal and parallel to [1 0 0], with dimensions 5.1 Å × 5.4 Å. Diffusion in the [0 0 1] direction is achieved by movement between these two channels [5].

The FCC feedstock is composed mainly by naphthenes, aromatics and alkanes. The study of naphthenes transformation, like methylcyclohexane, is particularly interesting because it allows a better understanding of the mechanisms of aromatics and coke formation [6–13]. However, the cracking chemistry of naphthenes is highly complex due to the high number of reactions occurring simultaneously: ring opening, hydride transfer, isomerization and cracking.

Besides hydrocarbons, FCC feedstocks contain metals, nitrogen and sulfur compounds that can have a deactivating effect. Although the damaging effect of the nitrogenated compounds has been known for several decades, the subject has not been studied to a great extent [14–28]. In the case of the specific deactivating effect over H-MFI zeolites, the lack of detailed studies is even higher. Nowadays, however, due to increasing level of impurities in the FCC feedstock, it constitutes a very relevant problem. The weight content of nitrogen in FCC feeds oscillates

* Corresponding author. Tel.: +351 21 841 9073; fax: +351 21 841 9198.
E-mail address: ramoa.ribeiro@ist.utl.pt (F.R. Ribeiro).

between 1200 and 1700 ppm. Molecules with small and medium molecular weight with well-defined structures were isolated from medium distillates. About 25–30% (400–600 ppm) are bases: pyridine, quinoline, isoquinoline, acridine and phenanthridine or alkyl derivatives of these compounds. The others are not basic and include normally a pyrrol nucleus: pyrrol, indole and carbazole.

Recently, we have reported the effect of quinoline on the methylcyclohexane transformation over H-USY zeolite [29]. In this work, the deactivation of HMFI zeolite was studied during the methylcyclohexane transformation at 350 °C in presence of three basic nitrogen compounds such as quinoline, 3-methyl and 2,6-dimethylpyridine. Furthermore, coke was analyzed during reaction. A temperature of 350 °C was chosen in order to enable a closer study of the coke formation reactions; at typical FCC riser temperatures (450–530 °C) the amount of analyzable coke (soluble in CH₂Cl₂) tends to be very low.

2. Experimental

The H-MFI zeolite was obtained by calcination of a NH₄-MFI zeolite (SM27, supplied by Alsi-Penta) under air flow at 500 °C for 12 h; its physicochemical properties are presented in Table 1.

The acidity of the samples was measured by adsorption of pyridine followed by IR spectroscopy, on a Nicolet 750 MAGNA-IRTM spectrometer. The samples were compressed into very thin wafers (5–15 mg/cm²). These wafers were then submitted to a pretreatment, in vacuum, during 1 h, at 200 °C. The chemisorption of pyridine (Sigma–Aldrich, IR spectroscopic grade) was done for 15 min at 150 °C with a large excess of nitrogenated base. The physisorbed pyridine was removed for 1 h under vacuum at the same temperature. In order to evaluate the strength of the acid sites, a stepwise desorption was done for the fresh H-MFI catalyst.

Nitrogen adsorption measurements were performed at 77 K with the gas adsorption system ASAP 2000 (Micromeritics). The microporous volume was estimated by the *t*-plot method using the Harkins and Jura standard isotherm. The external surface was determined by determination of the slope of *t*-plot curve in the *t* = 4–7.5 Å interval.

The catalytic tests were performed in a fixed-bed reactor at 350 °C and atmospheric pressure. A partial pressure of 1 × 10⁴ Pa of methylcyclohexane (Sigma–Aldrich, 99% pure) was used; nitrogen was the selected inert gas ($p_{\text{nitrogen}}/p_{\text{mch}} = 9$). The deactivation profile was obtained by taking samples of the reactor effluent for different values of times on stream (TOS): 1, 2, 5, 10, 15, 30 and 60 min. The first TOS value was selected

because it was the time necessary to obtain stable methylcyclohexane pressure. Several contact times were obtained by changing the mass of catalyst between 2 g and 75 mg. The contact time values were calculated as the inverse of weight hourly space velocity (WHSV). The reaction products were analyzed in a VARIAN 3400 chromatographer with a Plot Al₂O₃/KCl 50 m fused silica capillary column, using a flame ionization detector.

In the poisoning tests, 540 ppm of basic nitrogen was introduced in the reactor's feed. Three bases were selected: quinoline (Sigma–Aldrich, 99% pure), 2,6-dimethyl-pyridine (Sigma–Aldrich, 99% pure) and 3-methyl-pyridine (Sigma–Aldrich, 99% pure).

The main physicochemical properties of each one are presented in Table 2.

After reaction, the carbon and nitrogen contents of coke were analyzed by total combustion at 1050 °C with a mixture flow of helium and oxygen in a Thermoquest NA2100 analyzer.

The coke analysis was carried out by GC–MS coupling with a FINNIGAN INCOS 500 quadrupole mass spectrometer. To perform this analysis, it is necessary to separate completely the coke from the catalyst. To do so, a three-step procedure was used: first, the aluminosilicate matrix of the coked zeolite was dissolved in a HF solution (40%) at room temperature; secondly, the solution containing the coke molecules was neutralized with NaHCO₃; the third step consisted in a two-step extraction with CH₂Cl₂ [31–35]. The soluble coke is analyzed by the method mentioned above and the insoluble coke is recovered by filtration. Blank tests with typical coke molecules and all the three bases showed that the treatment caused no chemical changes on the carbonaceous compounds.

3. Results and discussion

3.1. Activity and deactivation

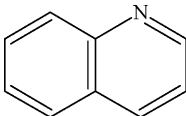
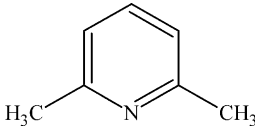
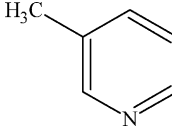
Even for methylcyclohexane alone, the activity of H-MFI zeolites decreases with the time-on-stream; this is due to the formation of polyaromatic compounds (coke) that stay trapped in the zeolites microporous structure. As it is visible in Fig. 1a, for a contact time of 12 min, the decrease is very strong for the first few minutes (0–5 min) after which the conversion stabilizes. The curve of carbon content versus TOS presents an almost identical profile (Fig. 1b). After a strong rate of coke production in the first few minutes of reaction, the amount of carbon deposited in the zeolite becomes constant (~1.5%). For the other contact times, the profiles are rather similar. Furthermore, the amount of

Table 1
Physicochemical properties of the H-MFI zeolite

Unit cell formula	Volume (cm ³ g ⁻¹)		Crystallites size (μm)	Amount of acid sites ^a (μmol g ⁻¹)					
	Micro	Meso		Brønsted			Lewis		
				150 °C	350 °C	450 °C	150 °C	350 °C	450 °C
H _{7.4} Al _{7.4} Si _{88.6} O ₁₉₂	0.151	0.016	1.0	1286	778	305	42	26	48

^a Acid sites able to retain pyridine under vacuum at 150, 350 and 450 °C.

Table 2
Physicochemical properties of the 3 nitrogen basic compounds

Nitrogen compound	Quinoline	2,6-Dimethylpyridine	3-Methylpyridine
Structure			
Boiling point (°C)	238	144	129
Protonic affinity ^a [30] (kJ/mol)	953	963	943
Kinetic diameter ^b (Å)	6.2	6.7	5.7
Molecular weight (g mol ⁻¹)	129.16	107.15	93.13
Amount in feed (wt.%)	0.50	0.42	0.36

^a The proton affinity can be define as the heat of reaction, at standard pressure and temperature, of the following reaction: $BH^+(g) + NH_3(g) \rightarrow NH_4^+(g) + B(g)$.

^b Kinetic diameter in relaxed conformation, calculated from *Cerius²* (*Biosym/Molecular Simulations*).

carbon trapped in the zeolite after 1 h does not differ significantly with contact time.

When nitrogen basic compounds are added to the reactor feed, for a contact time of 12 min, there is a strong increase in the deactivation with TOS (Fig. 1a). The first cause is undeniably the direct poisoning of the Brønsted acid sites. On the other hand, the

amount of carbon deposited in the zeolite after 1 h does not differ significantly with contact time. After 1 h, the injected amount of the three bases corresponds to carbon contents of 1.98, 2.01 and 2.15%, respectively, for 3-methylpyridine, 2,6-dimethylpyridine and quinoline. Adding these values to the carbon amount obtained without poisons, one can conclude that the augmentation in carbon content is primarily related with the retention of the bases.

The decrease in activity is enhanced for smaller contact times, when the ratio of injected basic molecules per mass of zeolites is higher. For high contact times, the mass of catalyst is so high that poisons have almost no effect in activity. The deactivation caused by each basic molecule for several contact times are presented in Table 3.

It is clear that the loss in activity is not the same for each one of the three bases. The poisoning ability of each base respects the following order: 2,6-dimethylpyridine > quinoline > 3-methylpyridine. Two explanations can be proposed: the amount of nitrogen deposited in the catalyst varies for the three bases or the effect of each poisoning molecule is different. By analyzing Fig. 2a, one comes to the conclusion that all the nitrogen introduced in the feed, which is equal for the three nitrogen bases, stays in the zeolite. Consequently, the differences in deactivation should be related to differences in the poisoning ability of each molecule. Obviously, there is a saturation amount of nitrogen ($\sim 0.8\%$) which corresponds to $710 \mu\text{mol g}^{-1}$. It is important to refer that the catalytic tests were carried out at a temperature lower than the industrial catalytic cracking one; reasons for this fact were mentioned earlier on. The question is to know if the deactivation observed here is significant at the typical FCC riser temperatures ($450\text{--}530^\circ\text{C}$) where desorption can be facilitated. Tests performed with quinoline at 450°C over demonstrated that nitrogen contents of 0.75% (carbon content of 9%) could be easily obtained after 1 h of reaction. The tests were carried out with 1090 ppm of basic nitrogen in the feed and $1/\text{WHSV} = 7$ min. The theoretical nitrogen content based in the injected amount is 0.85% which is only 13% higher than the measured value. Consequently, all the conclusions taken at 350°C seem to prevail at 450°C .

Several works conducted earlier for poisoning in Y zeolites also concluded that deactivation shown by catalysts was influenced by the physicochemical properties of the poisoning

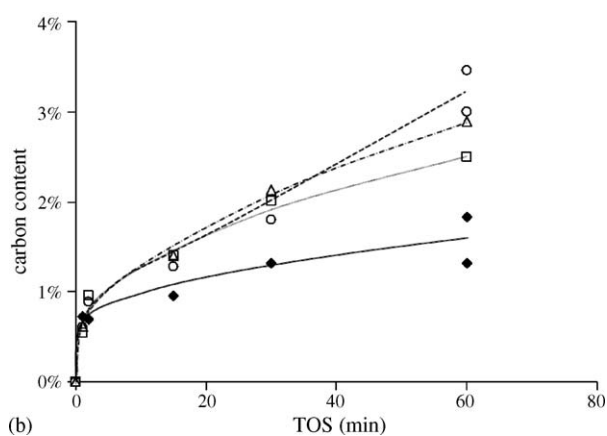
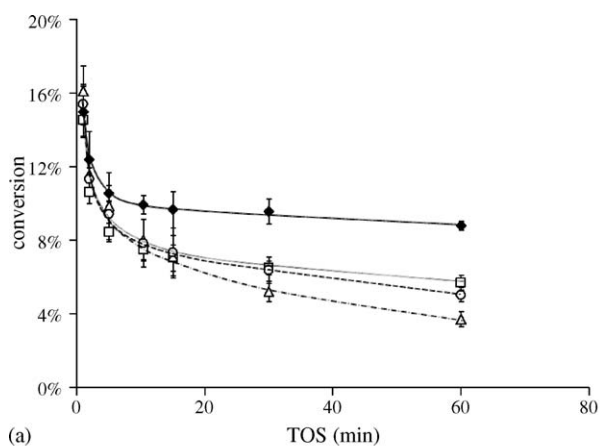


Fig. 1. (a) Conversion vs. TOS for a contact time of 12 min (the error bars correspond to the 95% confidence intervals calculated statistically) and (b) carbon content vs. time on stream for a contact time of 12 min. Tests performed with (◆) methylcyclohexane alone, (□) methylcyclohexane + 3-methylpyridine, (Δ) methylcyclohexane + 2,6-dimethylpyridine and (○) methylcyclohexane + quinoline.

Table 3
Activities (CSTR reactor model) and residual activities ($a_{TOS=60min}/a_{TOS=1min}$) for several contact times and nitrogen basic compounds

Reactant	Activities ($\text{mmol g}^{-1} \text{h}^{-1}$)	1/WHSV (min)			
		40	12	6	3
Methylcyclohexane alone	$a_{TOS=1min}$	11.3	11.8 ± 1.1	13.6	12.0
	$a_{TOS=60min}/a_{TOS=1min}$	0.66	0.59 ± 0.06	0.67	0.31
Methylcyclohexane + quinoline	$a_{TOS=1min}$	12.0	12.1 ± 0.9	11.9	12.0
	$a_{TOS=60min}/a_{TOS=1min}$	0.51	0.33 ± 0.05	0.11	0.05
Methylcyclohexane + 2,6-dimethylpyridine	$a_{TOS=1min}$	11.4	12.7 ± 1.1	13.5	12.4
	$a_{TOS=60min}/a_{TOS=1min}$	0.49	0.23 ± 0.04	0.08	0.02
Methylcyclohexane + 3-methylpyridine	$a_{TOS=1min}$	11.9	11.4 ± 0.7	11.6	12.0
	$a_{TOS=60min}/a_{TOS=1min}$	0.55	0.39 ± 0.04	0.19	0.05

nitrogen molecules. Recent works by Ho et al. [18] demonstrated that the poisoning ability of a nitrogen basic molecule could be determined by a balance between its molecular weight and protonic affinity (indicator of the basicity of the molecule). In this particular case, the observed poisoning abilities seem to correlate well with proton affinity values. If the amount of nitrogen

does not change, each basic molecule must, besides poisoning one acid site, cause a decrease in the acid strength of the neighbour acid sites. The extent of this reduction in acid strength is obviously related with the basicity of the poison, which explains the observed results. This theory had already been proposed by Corma and Mocholi [27] in the cracking of n-heptane over HY zeolites. If this effect really exists, it will be rather strong because the tested H-MFI zeolite presents a framework Si/Al ratio of 12, which is sufficiently high to assure that there are not acid sites in the direct proximities of each other.

In which concerns the molecular weight, quinoline, which is the heavier compound has a lower poisoning capacity than 2,6-dimethylpyridine, this seems to indicate that the basicity of the nitrogen compound is more important than its size. However, it is important to point out that 2,6-dimethylpyridine, although with a lower molecular weight, presents a higher kinetic diameter which can facilitate pore blockage. Nonetheless, this larger kinetic diameter can also difficult diffusion and consequently reduce the accessibility to the acid sites.

Fig. 2b shows the deactivation ($a_{mch+nitrogen}/a_{mch \text{ alone}}$) caused by each nitrogen base versus the amount of nitrogen deposited in the catalyst for equal values of TOS and contact time. For a given nitrogen base, the deactivation depends almost exclusively on the amount of nitrogen deposited in the zeolite. It is visible that for iso-nitrogen content the decrease in activity caused by the base respects the order of poisoning abilities already presented. A theoretical deactivation value was also determined (Fig. 2b), it was assumed that each injected basic molecule poisoned one Brønsted acid site able to retain pyridine at 150 °C. The deactivation calculated by this model is consistently lower than the experimental one, for all three nitrogen bases. It is important to refer that the determination of this theoretical value is based in three very questionable simplifications: (a) all Brønsted acid sites able to retain pyridine at 150 °C are supposed to be equally active in the methylcyclohexane transformation; (b) this prediction does not account the protonic sites blocked by coke; (c) all nitrogen molecules are assumed to adsorb onto Brønsted acid sites what is not necessarily true; the coordination with Lewis acid sites is also possible. Even so, the difference between theoretical and experimental values is consistent with the conclusion taken earlier on about the poisoning effect of each basic molecule.

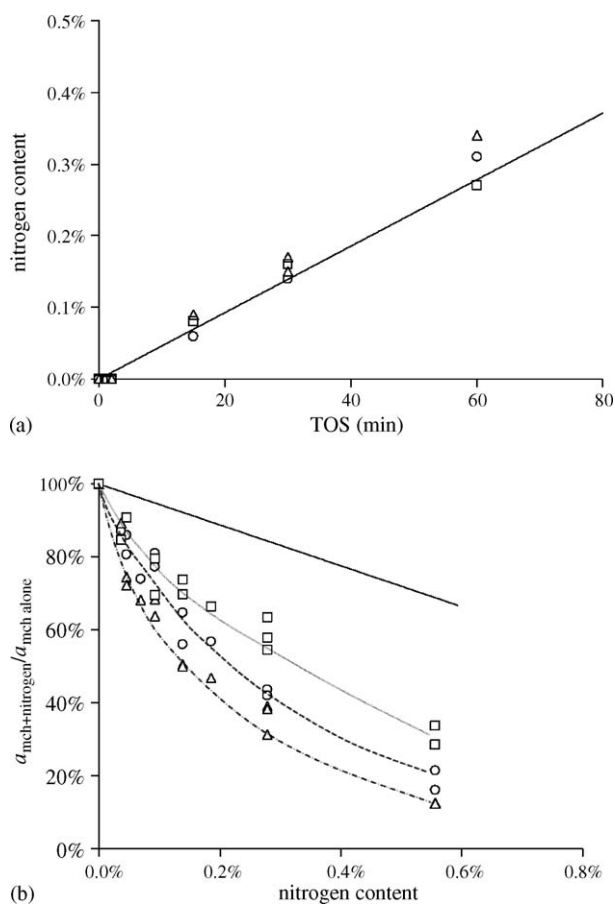


Fig. 2. (a) Nitrogen content vs. time on stream for a contact time of 12 min; (—) theoretical value of nitrogen content in the zeolite based in the injected amount and (b) activity loss due to poisoning by nitrogen molecules vs. nitrogen content; (—) theoretical loss in acid sites based in the injected quantity of quinoline and Brønsted acid sites density measured at 150 °C by pyridine adsorption. Tests performed with (□) methylcyclohexane + 3-methylpyridine, (Δ) methylcyclohexane + 2,6-dimethylpyridine and (○) methylcyclohexane + quinoline.

Fig. 2a shows that until a certain saturation limit, all the nitrogen molecules fed to the reactor stay in the zeolite. These results are somewhat surprising if one has into account that all three basic molecules have relatively large dimensions, specially 2,6-dimethylpyridine (Table 2). In fact, all three bases have molecular diameters larger than the aperture of the two types of channels existent in the MFI structure. The possibility that all the nitrogen bases would be retained in external surface is not credible. Studies show that for this crystallite size (1 μm) the relative amount of external sites is inferior than the amount correspondent to the observed saturation value in the tested H-MFI zeolite (710 $\mu\text{mol g}^{-1}$) [36]. In addition, a research work shown that 2,6-dimethylpyridine could be formed and diffused in the MFI structure pore system at 450 $^{\circ}\text{C}$ [37]. This means that all poison molecules must enter, to some extent, into the zeolite crystallites.

It is commonly accepted that molecules are primarily bound by dispersive interactions to the molecular sieve walls, independent of the presence or absence of Brønsted or Lewis acids sites. Molecules can “contract” to enter pores which have a size smaller (down to about 80%) than their free (gas phase) molecular size [38]. Similarly, the zeolite framework can be

distorted, at least locally, upon adsorption considering the magnitude of the physical interactions which are involved [38]. Such distortions or lattice relaxations have been reported experimentally upon adsorption of various molecules in MFI zeolites [39].

The extent of these distortions is proportional to the affinity between the zeolite and the adsorbing molecule. Due to its pronounced ionic nature, acid zeolites have a high affinity for polar molecules such as nitrogen bases. Obviously, the diffusion of the molecules in the zeolite channels is favored for higher temperatures. Afterwards, when the basic molecules reach the acid sites, the chemisorption occurs in almost irreversible form. In other words, the basic molecules are attracted by the zeolite polarity, diffuse in the interior of the micropores and stay trapped in the acid sites dispersed within these pores.

3.2. Product distribution

3.2.1. Fresh catalyst product distribution

Two types of products are formed during catalytic cracking reactions: coke and gas phase products. The principal

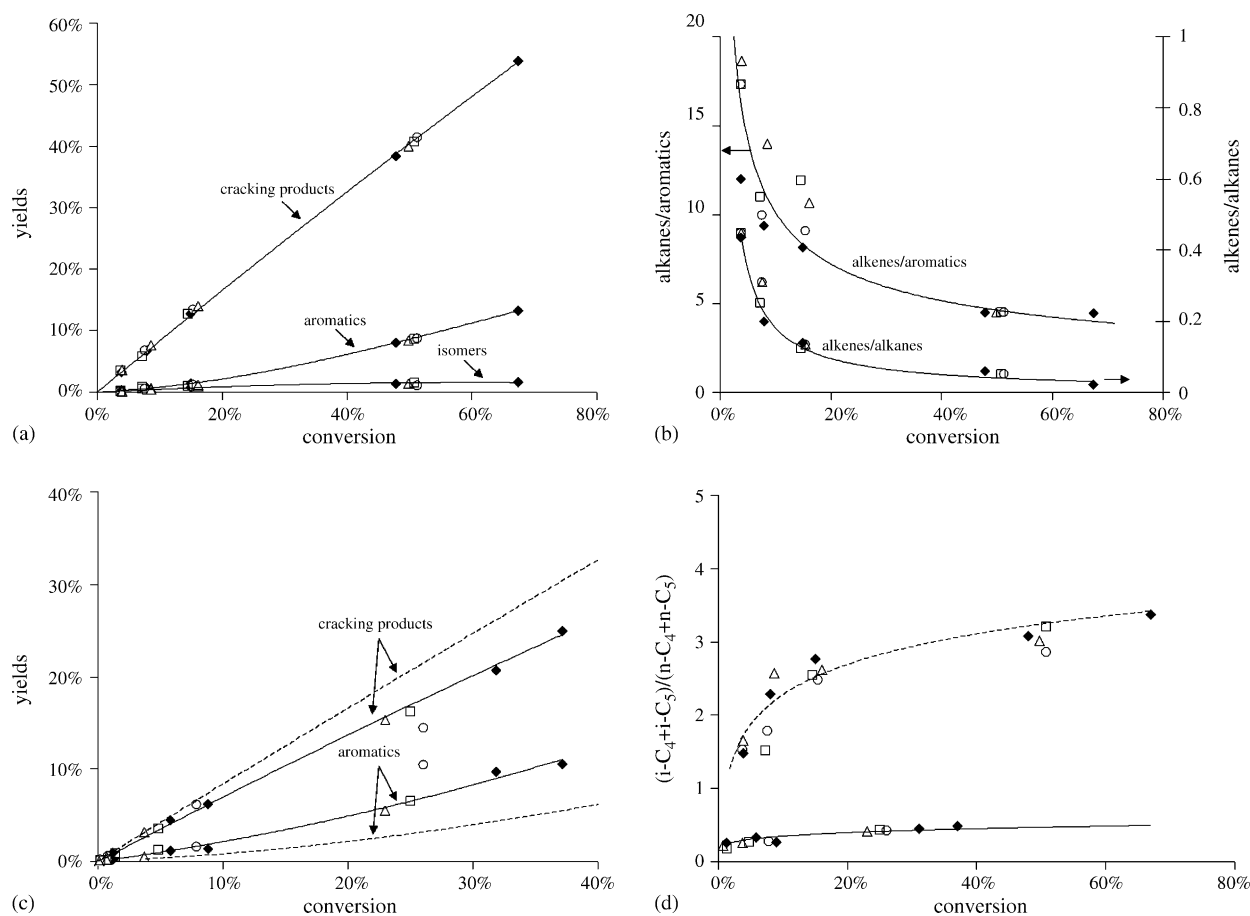
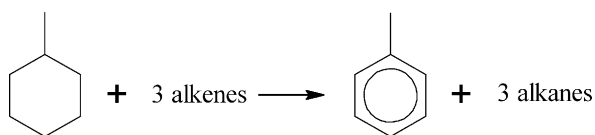


Fig. 3. (a) Initial yields (TOS=1 min) of cracking products, isomers and aromatics vs. conversion; (b) initial ratios (TOS=1 min) alkanes/alkenes and alkanes/aromatics vs. conversion; (c) yields for the coked zeolite (TOS=60 min) of cracking products and aromatics vs. conversion; (d) ratio $(i\text{-C}_4+i\text{-C}_5)/(n\text{-C}_4+n\text{-C}_5)$ vs. conversion. (c and d): (—) coked zeolite (TOS=60 min) and (---) “fresh” zeolite (TOS=1 min). Tests performed with (♦) methylcyclohexane alone, (□) methylcyclohexane + 3-methylpyridine, (Δ) methylcyclohexane + 2,6-dimethylpyridine and (○) methylcyclohexane + quinoline.

gas phase products of the transformation are C₃–C₆ alkanes obtained by β-scission cracking and C₇–C₈ aromatics; small amounts of C₂–C₄ alkenes and isomers (ethylcyclopentane and dimethylcyclopentanes) are also produced. The small quantity of methane and ethane produced are an indicator of the low importance of protolytic cracking for the given operating conditions. On the other hand, the low amount of produced isomers is not surprising if one considers the rather large size of dimethylcyclopentane isomers. The relatively narrow pores of the MFI structure must difficult the diffusion of these products.

Via β-scission mechanism, the cracking of methylcyclohexane should produce almost exclusively non-cyclic C₇ molecules by ring opening and C₃ and *i*-C₄ olefins by secondary cracking. However, products in C₅, C₆ and even C₈ are also produced in non-negligible amounts. They result from oligomerization reactions between adsorbed species and alkenes, forming by this route higher molecular weight compounds that can easily crack originating products other than C₃ and C₄.

Fig. 3a shows the initial yields in the three families (cracking products, aromatics and isomers); the predominance of cracking products is very clear. The behavior of the yield versus conversion curve is typical of primary products. On the other hand, aromatics are clearly secondary products. No visible differences exist between the tests carried out with the nitrogen bases and the tests performed with methylcyclohexane alone. The aromatics formation occurs by hydrogen transfer between the reactant and alkenes produced by cracking:



This last reaction causes a large consumption of alkenes which can be confirmed by the small value of the alkenes/alkanes ratio (Fig. 3b), specially for high conversions in agreement with the main production of alkanes as cracking products. For very small conversion values, the hydrogen transfer reaction is less favored and the alkenes/alkanes increases to values close to 0.5. Normally, and accordingly to the methylcyclohexane cracking stoichiometry, a reactant molecule should originate two alkenes. Therefore, even for low conversions, the production of aromatics is responsible for the consumption of two-third of the produced alkenes.

Having only this reaction into account, the alkanes/aromatics ratio should be equal to 3, however, aromatics can be converted into coke. This reaction is responsible by a strong consumption of aromatics for the first few minutes which induces a high increase in the alkanes/aromatics ratio (Fig. 3b). This phenomenon is more visible for low conversions. Although it is known that the production of coke is favored for high conversion, in reality carbon contents do not change much with conversion. The production of coke is so fast that for a given zeolite, after 1 min, the rate of coke formation is already strongly limited by the space available in the structure. On the other hand, as it is

visible in Fig. 3a, the selectivity in aromatics increases with conversion. This means that when the conversion is small, a larger fraction of the produced aromatics undergoes coke formation reactions.

3.2.2. Influence of coke in the product distribution

The catalytic properties of a MFI zeolite can be highly influenced by the coke deposited within its channels and intersections. The existence of coke can have the following effects: (a) increase of the diffusional limitations of the bulkier products, (b) intensification of the transition state shape selectivity inherent to this zeolite and (c) decrease in the Brønsted acid sites density. Besides, the selectivity in the families that participate in coke formation changes with the TOS, mainly because the amount of coke formed during the reaction is not constant. Fig. 3c shows the comparison of the yields in cracking products and aromatics for TOS = 1 and 60 min. It is perceptible that the aromatics yield augments and the yield in cracking decreases; the isomers yield is not significantly affected. The reason for these changes is evidently linked to coke formation; for TOS = 1, the formation of coke is very high while the same cannot be said for TOS = 60. As a consequence, the yield in aromatics is higher after 60 min of reaction. Obviously, if the yield in aromatics increases the yield in the other compounds, namely the cracking products, must decrease. Like for TOS = 1 min, no selectivity changes are noticed between tests performed with methylcyclohexane alone and with 540 ppm of basic nitrogen in the feed.

The accumulation of coke in the porous structure also causes changes in the ratio between branched and linear cracking products. Using the ratio $(i\text{-C}_4 + i\text{-C}_5)/(n\text{-C}_4 + n\text{-C}_5)$ as an indicator (Fig. 3d), it is clear that for the coked zeolite the production of linear products is favored due to an increase on the diffusional limitations of the branched ones. A similar effect is noticed for the production of aromatics. Normally, the MFI structure produces mainly 1,4-xylene because the 1,3-xylene and 1,2-xylene isomers cannot diffuse as easily as the first one. After coking, the diffusional limitations became even more pronounced and, consequently, the 1,4-xylene/(1,3-xylene + 1,2-xylene) ratio increases.

3.3. “Coke” characterization

In order to understand the chemistry behind coke formation and poisoning, the molecules retained during the reaction were analyzed by several characterization methods. The word coke is normally associated to heavy polyaromatic compounds; however, in this particular work the word coke in commas will be used for all molecules trapped in the zeolite.

3.3.1. Characterization in situ by FT-IR spectroscopy

By FTIR spectroscopy, one can analyze “coke” in situ both for the tests performed with methylcyclohexane alone and with nitrogen basic compounds. The vibration of the C–C conjugated bonds of the polyaromatics compounds have energies that correspond to the region of IR spectra between 1700 and 1300 cm⁻¹ (Fig. 4). For the samples without nitrogen several small inten-

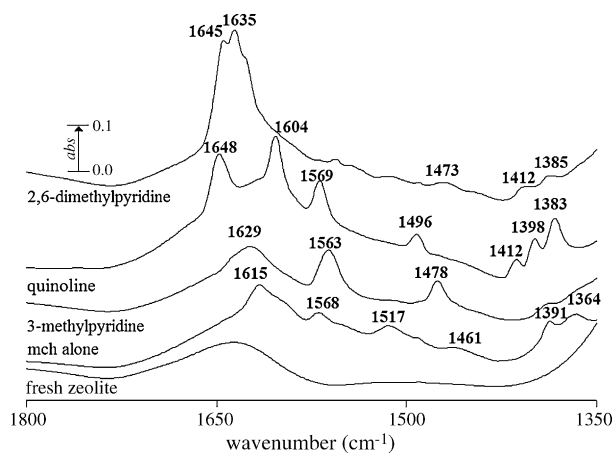


Fig. 4. IR spectra of the zeolite coked (contact time=12 min) with methylcyclohexane alone (%C=2.47); methylcyclohexane + 3-methylpyridine (%C=2.50); methylcyclohexane + quinoline (%C=2.89) and methylcyclohexane + 2,6-dimethylpyridine (%C=3.46).

sity bands are present, which is normal if one considers the small amount of “coke” deposited in the zeolite. The integrated surface of these bands is proportional to the amount of carbon measured by elemental analysis.

For the tests performed with nitrogen, besides the bands referred earlier on, there are other ones that appear in the same region of the spectra. For the samples containing 3-methylpyridine, three new bands are easily detectable: 1629, 1563 and 1478 cm^{-1} . No studies were found in literature about the adsorption of this base in zeolites.

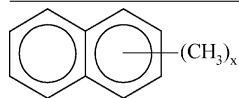
In zeolites poisoned with 2,6-dimethylpyridine, five new bands appear. The two intense bands positioned at 1635 and 1645 cm^{-1} agree fairly well with those reported in the literature for protonated species and they may be ascribed to vibration modes of 2,6-dimethylpyridinium species [40,41]. On the other hand, other less intense bands also appear at 1473, 1412 and 1385 cm^{-1} . These bands can also be seen in the IR spectra of physisorbed 2,6-dimethylpyridine; they are not characteristic from Lewis or Brønsted acid sites. The bands characteristic of coordination on Lewis acid sites (1618 and 1580 cm^{-1}) [40,41] are not visible.

For the tests performed with quinoline, the following bands appear: 1383, 1398, 1412, 1496, 1569, 1604 and 1648 cm^{-1} . The bands at 1412 and 1639 cm^{-1} are characteristic of quinoline molecules adsorbed in Brønsted acid sites [42,43]. Quinoline molecules coordinated with Lewis acid sites give origin to a band at 1516 cm^{-1} , in this case the band is imperceptible. The remaining bands are not characteristic of the interaction with neither one of the two types of acid sites, consequently they are less interesting.

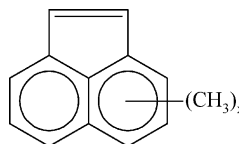
The intensity of all the above mentioned bands increases with the amount of nitrogen basic compounds in the zeolite. Curves of the amount of nitrogen injected for each value of TOS as a function of the more intense bands show an almost perfect linearity, thus supporting the fact that all quinoline injected stays retained in the zeolite. The bands characteristic of Lewis acid sites are not visible which seems to indicate that the basic molecules adsorb preferentially on the Brønsted acid sites. In addition, the amount of Lewis acid sites is very low.

Table 4
Coke molecules soluble in CH_2Cl_2 identified by GC–MS coupling

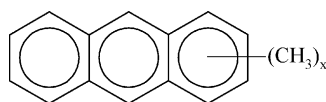
Soluble non-nitrogenated coke molecules formed in the H-MFI zeolite



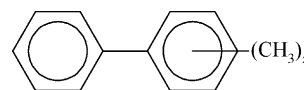
Methylnaphthalene ($x=1-4$), kinetic diameter^a = 6.2 Å,
MW = 128.17 + x 14 g mol^{-1}



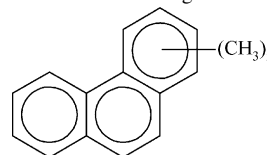
Methylacenaphthylene ($x=1-3$), kinetic diameter^a = 7.9 Å,
MW = 152.19 + x 14 g mol^{-1}



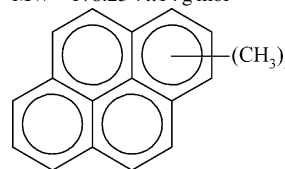
Methylantracene ($x=0-5$), kinetic diameter^a 6.2 Å,
MW = 178.23 + x 14 g mol^{-1}



Methylbiphenyl ($x=2-3$), kinetic diameter^a = 5.7 Å,
MW = 154.21 + x 14 g mol^{-1}



Methylphenanthrene ($x=0-5$), kinetic diameter^a = 6.2 Å,
MW = 178.23 + x 14 g mol^{-1}



Methylpyrene ($x=1-3$), kinetic diameter^a = 7.9 Å,
MW = 202.25 + x 14 g mol^{-1}

^a Kinetic diameter without CH_3 in relaxed conformation, calculated from Cerius² (Biosym/Molecular Simulations).

3.3.2. Identification of the constituents of “coke” by GC–MS coupling

As described earlier, after the reaction, the zeolite matrix was dissolved with HF and the organic coke molecules were recovered by liquid–liquid extraction. The GC–MS coupling allowed identification of the soluble coke molecules formed in the MFI structure during the methylcyclohexane transformation at 350 °C. For a given zeolite structure, “coke” composition changes with several factors: contact time, TOS, presence of impurities, temperature, reactant partial pressure, etc. In this particular case, only two of these items were studied: TOS and presence of impurities. For the zeolites with higher coke contents, a part of coke was insoluble in the organic phase; the quantification was not possible due to low amounts of “coke” formed with this zeolite at the selected reaction conditions.

The intersection of the two types of channels of the MFI zeolite results in structures with 8–9 Å for H-MFI [44]. Therefore, “coke” molecules with larger sizes cannot be formed within the microporous network. Larger molecules, normally insoluble, can form on the crystallites external surface but cannot be analyzed.

Whatever the reaction conditions (with and without nitrogen bases in the feed), the detected hydrocarbonated “coke” molecules soluble in CH₂Cl₂ are presented in Table 4. In the presence of nitrogen bases, no nitrogen containing “coke” molecules, other than the injected bases, were detected for neither one of the samples. It is important to refer that for high TOS values, in the tests carried out with nitrogen, the basic molecules were always the principal constituent of “coke”. In which regards the non-nitrogenated “coke” molecules, for smaller TOS values, the principal constituents were methyl substituted naphthalenes, anthracenes and phenanthrenes. On the other hand, for high TOS values the family of pyrenes was the principal constituent. These last ones are the bulkier molecules formed at these conditions, they present a size similar to those of the channels intersections (8–9 Å).

The inexistence of other nitrogen “coke” molecules, other than the bases, confirms that none of them undergo easily reactions with superficial charged species. This reaction is very improbable comparatively to the adsorption onto the Brønsted acid sites. The principal reason is the electronegativity of the nitrogen atom; it retains a pair of electrons making the nitrogening a π -electron deficient system which is highly deactivated towards electrophilic substitutions. Even so, quinoline molecule is the less deactivated because a high resonance stabilization can be achieved, by substituting in position 2, without introducing any positive charge in the nitrogen atom. Previous works showed that the electrophilic substitution of quinoline could be easily performed over H-Y zeolites at 350 °C [45,46]. Furthermore, our previous works with an H-USY zeolite and quinoline [29] demonstrated that the reaction occurred, specially when the amount of available acid sites was low. In this case, for a contact time of 12 min and TOS=60 there are still some activity which is indicative of the presence of some acid sites. Maybe if the coke was analyzed after complete deactivation, some nitrogen coke compounds, other than actual bases, would be found.

3.3.3. Evolution of the microporous volume and external surface measured by N₂ adsorption

The measurement of the reduction of microporous volume with coking is very important in this particular zeolite due to its narrow pores which can be easily blocked. As it is visible in Fig. 5a, the pore blockage increases in almost linear fashion with the amount of carbon deposited in the catalyst. It seems that the decrease in accessible volume is higher for the tests performed with the nitrogen bases, however; the comparison made for the highest carbon contents values has some limitations due to the fact that TOS values are not the same (1 h versus 4 h).

Analyzing the zeolite external surface (Fig. 5b) one also obtains interesting results. A strong decrease in the crystallites external surface during the reaction was observed which seems to imply that the blockage of the pores mouth is one of the causes of deactivation. Furthermore, differences are noticed between the zeolites coked with methylcyclohexane alone and with each one of the nitrogenated bases. To begin with, in the tests carried out with methylcyclohexane alone the decrease in external surface seems to be lower. On the other hand, for the tests performed with bases, 2,6-dimethylpyridine seems to clearly have a larger impact in the external surface reduction comparatively to the other two bases. As it was presented earlier on (Table 2),

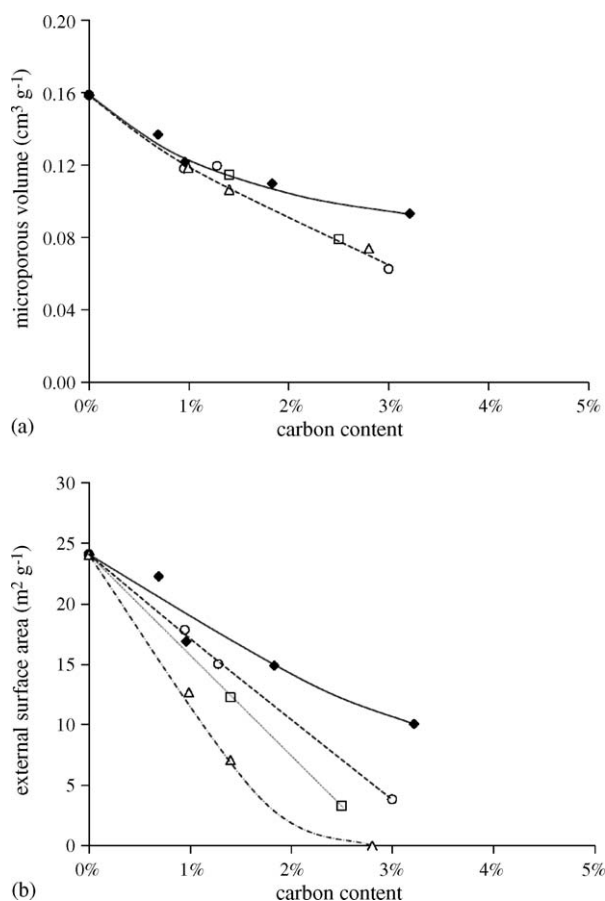


Fig. 5. (a) Microporous volume vs. carbon content for a contact time of 12 min and (b) external surface vs. carbon content for a contact time of 12 min. Tests performed with (◆) methylcyclohexane alone, (□) methylcyclohexane + 3-methylpyridine, (Δ) methylcyclohexane + 2,6-dimethylpyridine and (○) methylcyclohexane + quinoline.

the referred base is the bulkier one having a kinetic diameter considerably higher than the MFI zeolite pores aperture. As it was said above, 2,6-dimethylpyridine can penetrate into the MFI porous structure at high temperatures. Despite this fact, it is completely understandable that 2,6-dimethylpyridine has tendency to penetrate less in the crystallites and accumulate in the external surface. In which regards the other two bases, no major differences are found.

3.4. Evolution of acidity measured by FT-IR spectroscopy

Two distinct –OH vibration bands are present in the IR spectrum of the H-MFI zeolite, one at 3613 cm^{-1} which corresponds to the Al–OH–Si acid groups and another at 3744 cm^{-1} which can be associated to the Si–OH groups present in framework defects and crystallites external surface. Although all Al–OH–Si groups are potentially active, its accessibility must also be assessed. To do so, one can adsorb a basic compound and account by FTIR spectroscopy the decrease in the bands corresponding to –OH groups; all the accessible ones will be occupied by the base and will stop vibrating; by subtraction one can determine the relative amount of accessible –OH acid groups. Pyridine was chosen as the probe molecule for several reasons; one of them

is its size which is roughly comparable to the one of the reactant molecule. Basically, this means that the acid sites accessible to pyridine will be also accessible to methylcyclohexane. Fig. 6a shows, as an example, the spectra of the fresh H-MFI zeolite and two samples coked with methylcyclohexane alone (15 min and 4 h), before and after pyridine adsorption. It is visible that for the fresh zeolite all Al–OH–Si groups are acid and accessible to pyridine; contrarily, Si–OH groups are not acid. On the other hand, for the coked zeolite some of the existent acid sites are blocked and cannot interact with pyridine. Furthermore, after 4 h of reaction, there are some free Al–Si–OH groups but none of them are accessible to pyridine. However, after 4 h (%C = 2.47) of reaction the zeolite presents yet a small activity. In which regards the Si–OH groups, while after 15 min (%C = 0.96) the reduction of the band is very small, after 4 h (%C = 2.47) the band disappears completely which agrees with the existence of insoluble coke for this sample.

Normally, the most used method to determine the acidity of a zeolite is to adsorb a basic molecule and measure the intensity of the bands correspondent to interaction of this base with the acid sites. In this particular case, when pyridine is adsorbed, two intense bands appear corresponding to pyridinium ions (1545 cm^{-1}) and pyridine bonded to Lewis

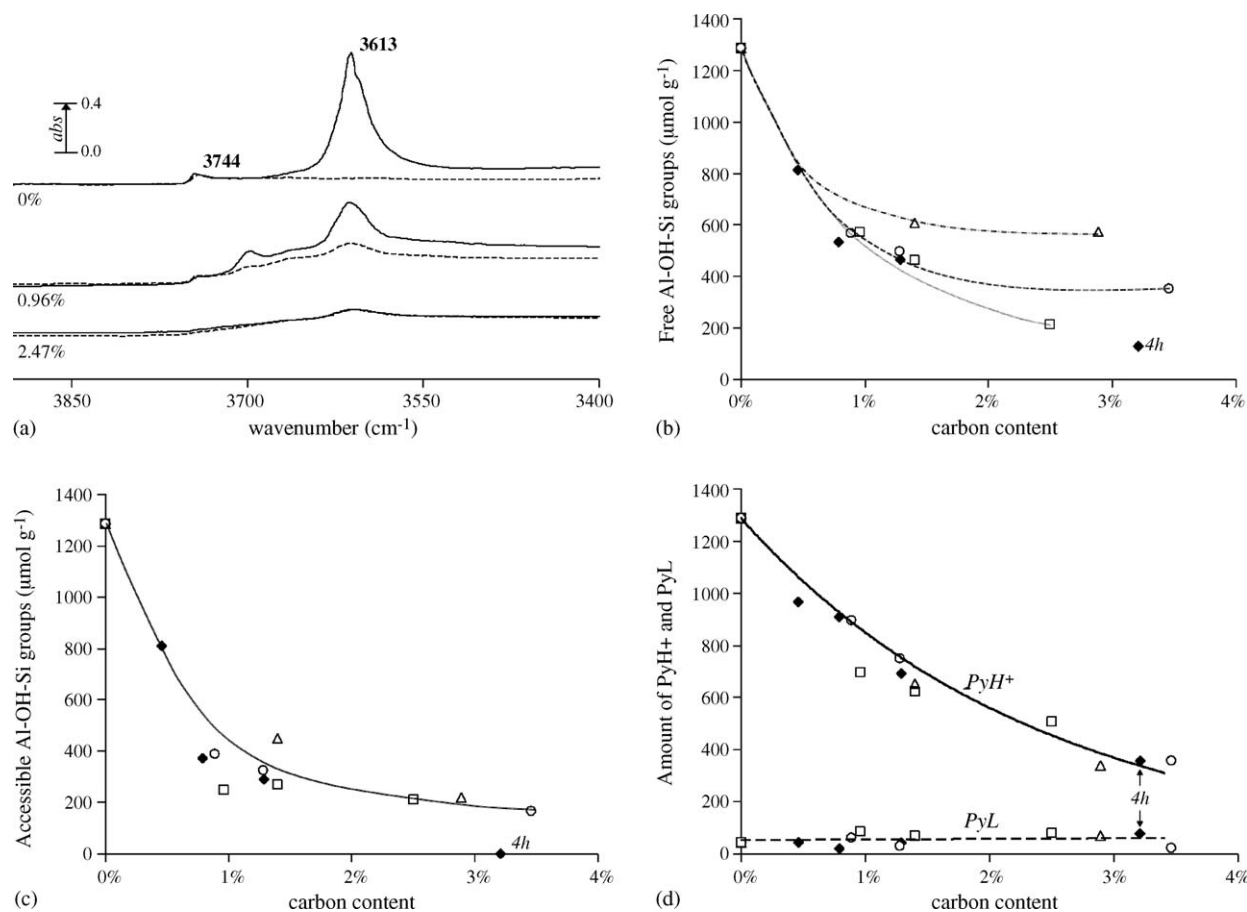


Fig. 6. (a) IR spectra of the fresh zeolite and of the zeolite coked with methylcyclohexane alone for two carbon content values (TOS = 15 min and 4 h) showing the bands corresponding to acid Al–OH–Si and Si–OH groups (—) accessible and (---) inaccessible to pyridine at 150 °C; (b) amount of free (vibrating) Al–OH–Si groups vs. carbon content; (c) amount of Al–OH–Si groups accessible to pyridine at 150 °C vs. carbon content; (d) amount of (—) pyridinium ions and (---) pyridine molecules coordinated with Lewis acid sites vs. carbon content. Tests performed with (♦) methylcyclohexane alone, (□) methylcyclohexane + 3-methylpyridine, (Δ) methylcyclohexane + 2,6-dimethylpyridine and (○) methylcyclohexane + quinoline.

acid sites (1450 cm^{-1}). The extinction coefficients are well known, 1.13 and $1.28\text{ cm}^2\text{ }\mu\text{mol}^{-1}$, respectively, for Brønsted and Lewis acid sites [47,48]. For the fresh catalyst all the Al–OH–Si groups are accessible; furthermore, no “coke” is present which means that only the Al–OH–Si groups can protonate pyridine. Consequently, the amount of pyridinium ions observed at $150\text{ }^\circ\text{C}$ would be the same that those of Al–OH–Si groups. Based on this fact, a relation between the number of acid sites and the intensity of the band at 3613 cm^{-1} can be established.

Fig. 6b shows the evolution of total free Al–OH–Si groups during the reaction; it is noticeable that largest consumption of acid sites occurs in the first minutes of the reaction, for small carbon content values. Afterwards, the concentration of free Al–OH–Si groups decreases less with carbon content. Interestingly, the three bases do not seem to occupy the same number of acid sites. The stronger poison, 2,6-dimethylpyridine, is even the one for which the amount of free acid sites is highest, followed by quinoline and 3-methylpyridine in that order. Previously, it was shown that the amount of nitrogen base in the zeolite was the same for a given TOS value. This result do not seem to agree with this fact, in addition, why does 2,6-dimethylpyridine poison more than the other bases if the amount of free acid sites is higher with this base. Earlier, it was referred that 2,6-dimethylpyridine was the bulkier base and probably could not penetrate as deep into crystallites as the other two bases, as the N_2 adsorption results later confirmed. This means that this particular base probably cannot reach the acid sites present deep into the crystallite, which would explain the larger amount of free acid sites.

On the other hand, by analyzing of the evolution of the amount of Al–OH–Si groups accessible to pyridine with carbon content, it is observable that there are no major differences for the three bases (Fig. 6c). Consequently, the ratio of accessible acid sites per total number of acid sites is smaller for 2,6-dimethylpyridine.

The other way of expressing the decrease in acidity during the reaction is to quantify the decrease in the 1545 cm^{-1} band after pyridine adsorption. In order to perform this quantification, an extra factor had to be taken into line of account: there might be some exchange between the probe molecule (pyridine) and the poisoning bases. The basicity of pyridine in the gas phase ($\text{PA}_{\text{pyridine}} = 930\text{ kJ/mol}$) is lower than the basicity of either one of the three tested nitrogen bases (Table 2), however, the poison molecules is present in a large excess what can shift the equilibrium enabling the substitution. Consequently, the amount of pyridinium ions in the catalyst is always somewhat overestimated comparatively to the real value. To determine the real amount of pyridinium ions formed in the zeolite during the reaction, one must also have into account the diminution of intensity of the bands corresponding to each one of the protonated bases. The single case where a decrease was noticed was for 3-methylpyridine, i.e., the weakest base. Having into line of account the decrease in 1478 cm^{-1} band and the amount of 3-methylpyridine initially present in the catalyst, it is possible to determine the excess pyridinium ion. The total amount of pyridinium ions should be calculated as the quantity determined by the 1545 cm^{-1} band intensity minus the observed decrease in the

amount of 3-methylpyridinium ions when the pyridine molecule was added.

One would expect that the representation of the number of pyridinium ions (Fig. 6c) versus coke content would have the same evolution as the amount of accessible Al–OH–Si groups. Surprisingly, the amount of formed pyridinium ions is always higher than the amount of accessible Al–OH–Si groups. Two justifications can be pointed out to explain this behavior: (a) the basic pyridine molecules remove the lighter coke molecules from acid sites replacing them and (b) the pyridine molecules protonate in the charged coke molecules adsorbed on the acid sites. Both are plausible explanations for the observed phenomenon; in either case the amount of Brønsted acid sites is overestimated relatively to the real value. In which concerns the Lewis acidity, no significant changes are visible during the reaction. It seems that poisons really have a larger affinity towards the Brønsted acid sites.

A synthetic view of the deactivation mode of H-MFI catalyst during methylcyclohexane transformation in presence of various nitrogen molecules can be illustrated in Fig. 7. While for a bulky base molecule, the diffusion is more difficult and poisoning occurs mostly in the outer shell of the crystallite, for a smaller base poisoning happens uniformly through the microporous structure. As a consequence, in the first case (Fig. 7a) the

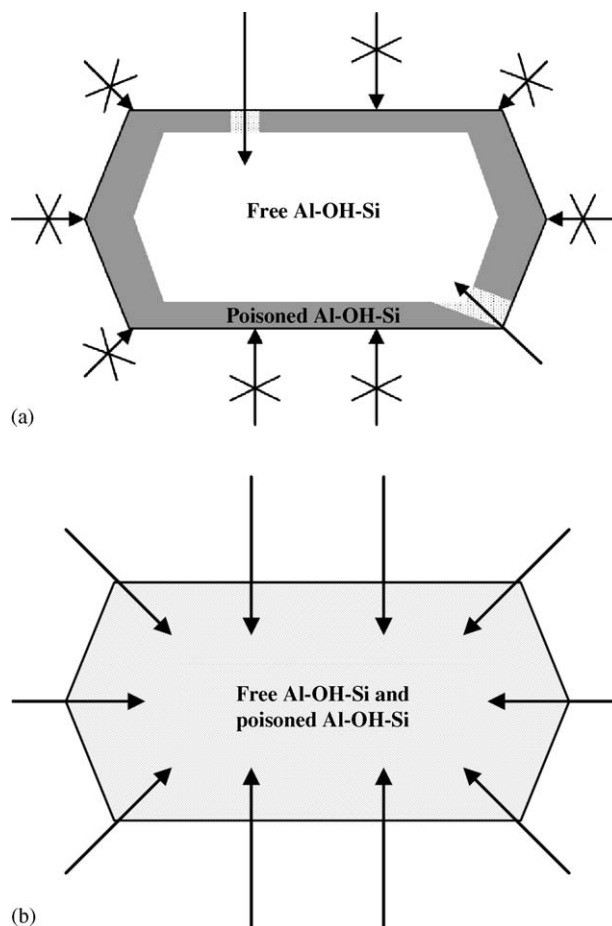


Fig. 7. (a) Selective poisoning of the crystallites outer shell and (b) uniform poisoning of the zeolite crystallite.

amount of free acid sites is higher because only a part of the acid sites were accessible. However, due to the accumulation of poison molecules in pore mouth, the diffusion of the reactant molecules, in this case represented pyridine, is very difficult and the relative amount of accessible acid sites is low. Despite this fact, the pore aperture blockage is not complete because some methylcyclohexane molecules continue to be able to react, hence the conversion exhibited after 1 h of reaction. On the other hand, when the basic molecule is smaller and poisoning occurs in a uniform way (Fig. 7b), the amount of vibrating Al–OH–Si groups is lower but the diffusion of reactant (or probe molecule) is easier what makes the relative amount of accessible acid sites larger.

4. Conclusions

The activity of the tested H-MFI zeolite for the transformation of methylcyclohexane is clearly influenced by the presence of basic nitrogen molecules. The decrease in conversion is due to the almost irreversible interaction of the basic molecules with the Brønsted acid sites responsible for the reaction. Besides, the bulky nitrogen bases stay in the micropores, increasing diffusional limitations and decreasing activity. The basic nitrogen compounds have a cumulative effect, the deactivation increases with amount of nitrogen deposited in the catalyst. Consequently, the referred effect is enhanced with the decrease of the contact time and with the increase of the TOS.

All the basic nitrogen introduced in the feed are retained in the Brønsted acid sites until a given saturation limit. Despite the fact that all bases have kinetic diameters higher than the aperture of the MFI zeolite micropores, the basic molecules seem to be able to enter the porous system. Nonetheless, for the bulkier bases the diffusion seems to be more difficult, consequently they penetrate less into the zeolites crystallites. The poisoning ability of each base seems to be related with its proton affinity. The intrinsic poisoning power of the bases respects the following order: 2,6-dimethylpyridine > quinoline > 3-methylpyridine.

The constituents of “coke” were analyzed by GC–MS coupling; no nitrogen other than the bases itself were found in the zeolite. The nitrogen atom in the aromatic ring of basic molecules deactivates it for electrophilic substitution reactions. This means that the nitrogen aromatic compounds do not act as coke precursors unlike other aromatics.

By FT-IR spectroscopy, it was possible to follow the acidity of the samples during the reaction, for the tests carried with and without nitrogen bases. No difference was found in the amount of free accessible Brønsted acid sites for the three bases. Therefore, the difference in the poisoning ability of each base should be linked to an inductive deactivation effect of the neighbor sites.

Acknowledgments

The first author expresses his gratitude to the Fundação para a Ciência e Tecnologia (FCT) for its monthly financial support (ref. SFRH/BD/13411/2003). Besides, all authors thank the Fundação para a Ciência e Tecnologia (FCT) for financing the project ref. POCI/EQU/58550/2004.

References

- [1] R.J. Madon, *J. Catal.* 129 (1991) 275.
- [2] J.S. Buchanan, J.G. Santiesteban, W.O. Haag, *J. Catal.* 158 (1996) 279.
- [3] C. Liu, Y. Deng, Y. Pan, Y. Gub, B. Qiao, X. Gao, *J. Mol. Catal. A* 215 (2004) 195.
- [4] M.A. den Hollander, M. Wissink, M. Makkee, J.A. Moulijn, *Appl. Catal. A Gen.* 223 (2002) 85.
- [5] D.H. Olson, G.T. Kokotailo, S.L. Lawton, *J. Phys. Chem.* 85 (1981) 2238.
- [6] W.C. Cheng, K. Rajagopalan, *J. Catal.* 119 (1989) 354.
- [7] A. Corma, F. Mocholi, V. Orchilles, G.S. Koermer, R.J. Madon, *Appl. Catal.* 67 (1991) 307.
- [8] E.F. Sousa-Aguiar, C.J.A. Mota, M.L.M. Valle, M.P. da Silva, D.F. da Silva, *J. Mol. Catal. A* 104 (1996) 267.
- [9] G. de la Puente, U. Sedran, *Appl. Catal. A Gen.* 144 (1996) 147.
- [10] A. Corma, F. Mocholi, V. Orchillés, *Appl. Catal.* 67 (1990) 307.
- [11] H.S. Cerqueira, P.C. Mihindou-Koumba, P. Magnoux, M. Guisnet, *Ind. Eng. Chem. Res.* 40 (2001) 1032.
- [12] A. Corma, A.L. Agudo, *React. Kinet. Catal. Lett.* 16 (1981) 253.
- [13] P.C. Mihindou-Koumba, H.S. Cerqueira, P. Magnoux, M. Guisnet, *Ind. Eng. Chem. Res.* 40 (2001) 1042.
- [14] G.A. Mills, E.R. Boedecker, A.G. Oblad, *J. Am. Chem. Soc.* 72 (1950) 1554.
- [15] P.A. Jacobs, C.F. Heylen, *J. Catal.* 34 (1974) 267.
- [16] P.A. Jacobs, H.E. Leeman, J.B. Uytterhoeven, *J. Catal.* 33 (1974) 17.
- [17] G. Caeiro, P. Magnoux, J.M. Lopes, F. Lemos, F. Ramôa Ribeiro, *J. Mol. Catal. A* 249 (2006) 149.
- [18] T.C. Ho, A.R. Katritzky, S.J. Cato, *Ind. Eng. Chem. Res.* 31 (1992) 1589.
- [19] R. Hughes, G. Hutchings, C.L. Kloon, B. McGhee, C.E. Snape, D. Yu, *Appl. Catal. A Gen.* 144 (1996) 269.
- [20] R. Hughes, G. Hutchings, C.L. Kloon, B. McGhee, C.E. Snape, in: B. Delmon, G.F. Froment (Eds.), *Catalyst deactivation*, *Stud. Surf. Sci. Catal.* 88 (1994) 377.
- [21] S.E. Voltz, D.M. Nace, M.J. Solomon, V.W. Weekman, *Ind. Eng. Chem. Proc. Des. Dev.* 11 (1972) 261.
- [22] S.M. Jacob, B. Gross, S.E. Voltz, V.W. Weekman, *AIChE J.* 22 (1976) 701.
- [23] R.F. Schwab, K. Baron, 2nd Katalistiks FCC Symposium, Amsterdam, 1981.
- [24] C.-M. Fu, A.M. Schaffer, *Ind. Eng. Chem. Prod. Res. Dev.* 24 (1985) 68.
- [25] J. Messrs, J. Scherzer, D.P. McArthur, Paper Presented at the NPRA Meeting Held on March 23–26, 1986.
- [26] J. Scherzer, D.P. McArthur, *Ind. Eng. Chem. Res.* 27 (1988) 1571.
- [27] A. Corma, F.A. Mocholi, *Appl. Catal. A Gen.* 84 (1992) 31.
- [28] Y. Briker, Z. Ring, A. Iacchelli, N. McLean, *Fuel* 82 (2003) 1621.
- [29] G. Caeiro, P. Magnoux, J.M. Lopes, F. Ramôa Ribeiro, *Appl. Catal. A Gen.* 292 (2005) 189.
- [30] E.P. Hunter, S.G. Lias, *J. Phys. Chem. Ref. Data* 27 (1998) 413.
- [31] M. Guisnet, P. Magnoux, *Appl. Catal.* 54 (1989) 1.
- [32] M. Guisnet, P. Magnoux, in: B. Delmon, G.F. Froment (Eds.), *Catalyst deactivation*, *Stud. Surf. Sci. Catal.* 88 (1994) 53.
- [33] S. Gnep, M. Guisnet, *Catal. Today* 31 (1996) 275.
- [34] M. Guisnet, P. Magnoux, D. Martin, in: B.C.H. Bartholomew, G.A. Fuentes (Eds.), *Catalyst Deactivation*, *Stud. Surf. Sci. Catal.* 111 (1997) 1.
- [35] M. Guisnet, P. Magnoux, *Appl. Catal. A Gen.* 212 (2001) 83.
- [36] S. Melson, F. Schüth, *J. Catal.* 170 (1997) 46.
- [37] F. Van der Gaag, R. Adriaansens, H. Bekkum van, P. van Geem, *Stud. Surf. Sci. Catal.* 49 (1990) 283.
- [38] E.G. Derouane, *J. Mol. Catal. A* 134 (1998) 29.
- [39] E.L. Wu, S.L. Lawton, D.H. Olson, A.C. Rohrman Jr., G.T. Kokotailo, *J. Phys. Chem.* 83 (1979) 7979.
- [40] C. Morterra, G. Cerrato, G. Meligrana, *Langmuir* 17 (2001) 7053.
- [41] T. Onfroy, G. Clet, M. Houalla, *Microporous Mesoporous Mater.* 82 (2005) 99.

- [42] T.J. Dines, L.D. MacGregor, C.H. Rochester, *Langmuir* 18 (2002) 2300.
- [43] A. Corma, V. Fornés, F. Rey, *Zeolites* 12 (1993) 56.
- [44] E.G. Derouane, Z. Gabelica, *J. Catal.* 65 (1980) 486.
- [45] P. Ram Reddy, K.V. Subba Rao, M. Subrahmanyam, *Catal. Lett.* 56 (1998) 155.
- [46] P. Ram Reddy, M. Subrahmanyam, V. Durga Kumari, *Catal. Lett.* 60 (1999) 161.
- [47] M. Guisnet, P. Ayrault, J. Datka, *Pol. J. Chem.* 71 (1997) 1455.
- [48] M. Guisnet, P. Ayrault, C. Coutanceau, M.F. Alvarez, J. Datka, *J. Chem. Soc. Faraday Trans.* 93 (1997) 1661.